

Structure-based design, synthesis, and SAR evaluation of a new series of 8-hydroxyquinolines as HIF-1 α prolyl hydroxylase inhibitors

Namal C. Warshakoon,* Shengde Wu, Angelique Boyer, Richard Kawamoto, Justin Sheville, Sean Renock, Kevin Xu, Matthew Pokross, Songtao Zhou, Carol Winter, Richard Walter, Marlene Mekel and Artem G. Evdokimov

Drug Discovery Division, Procter and Gamble Pharmaceuticals Inc., 8700 Mason-Montgomery Road, Mason, OH 45040, USA

Received 11 July 2006; revised 7 August 2006; accepted 8 August 2006

Available online 22 August 2006

Abstract—A new series of potent 8-hydroxyquinolines was designed based on the newly resolved X-ray crystal structure of EGLN-1. Both alkyl and aryl 8-hydroxyquinoline-7-carboxyamides were good HIF-1 α prolyl hydroxylase (EGLN) inhibitors. In subsequent VEGF induction assays, these exhibited potent VEGF activity. In addition, this class of compounds did show the ability to stabilize HIF-1 α .

© 2006 Elsevier Ltd. All rights reserved.

Hypoxia inducible factor (HIF) is a transcriptional complex that plays a key role in mammalian oxygen homeostasis and activates a host of hypoxic response genes that regulate angiogenic, glycolytic, and erythropoietic processes.^{1–3} The subunit components, HIF-1 α and HIF-1 β (ARNT), are constitutively expressed and regulation is achieved by the selective destruction of HIF-1 α . HIF-1 α is a major control element of the cellular response to hypoxia (low partial pressure of oxygen).

A family of non-heme iron-containing prolyl hydroxylases (EGLN-1, EGLN-2, EGLN-3) effects post-translational modification of HIF-1 α . In a reaction requiring Fe²⁺, oxygen, and ascorbate, these prolyl hydroxylases catalyze the oxidative decarboxylation of 2-oxoglutarate (2-OG) and the hydroxylation of proline⁵⁶⁴ and proline⁴⁰² in the oxygen-dependent degradation domain (ODDD) of HIF-1 α .^{4–6} Proline hydroxylation then targets HIF-1 α for proteasomal degradation via binding to the VHL (Von Hippel Lindau tumor suppressor protein), elongin C/B, Cul2, Rbx1 ubiquitin ligase complex.

Since this hydroxylation of HIF-1 α is strictly dependent on oxygen concentration; under hypoxia this reaction is inhibited, and the surviving HIF-1 α binds to ARNT to form a functional transcriptional activator that turns on genes with hypoxic response elements (e.g., VEGF, EPO, and glycolytic enzymes).⁷ Therefore, inhibition of HIF-1 α prolyl hydroxylases, resulting in HIF-1 α stabilization, has the potential to be a viable therapeutic approach for ischemic diseases including myocardial infarction, stroke, peripheral arterial disease, heart failure, diabetes, and anemia.

In the recent years, some small molecule HIF-1 α inhibitors have emerged as possible therapeutics for ischemic diseases.⁸ These are small ‘peptide-like’ molecules (e.g., **1** and **2**) that resemble 2-oxoglutarate (2-OG). One example, isoquinoline **3**, acts as a 2-oxoglutarate mimetic and thus exerts prolyl hydroxylase inhibition (IC₅₀: 1.4 μ M in our EGLN-1 assay) (Fig. 1).⁹

Our goal was to design novel HIF-1 α prolyl hydroxylase inhibitors based on the recently solved X-ray crystal structure of the complex between catalytic domain of EGLN-1 and the isoquinoline **3**.¹⁰ The isoquinoline nitrogen and the amide carbonyl interact with iron, while the phenolic OH and the amide NH are involved in hydrogen bonding interactions that impose structural rigidity to the molecule. The side-chain carboxylate

Keywords: Prolyl hydroxylase inhibitors; HIF-1 α ; Hypoxia; Ischemia; Peripheral arterial disease (PAD); Anemia; 8-Hydroxyquinolinecarboxyamides.

* Corresponding author. Tel.: +1 513 622 2284; fax: +1 513 622 0523; e-mail: Warshakoon.nc@pg.com

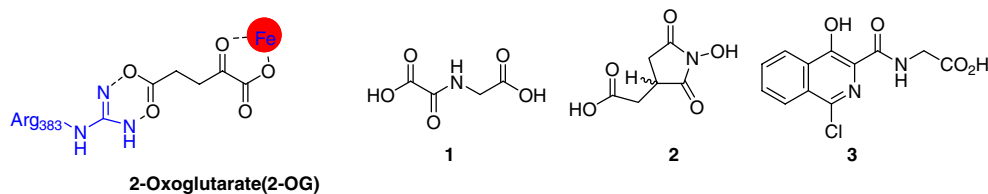


Figure 1. Small molecule HIF-1 α prolyl hydroxylase inhibitors.

reaches toward Arg³⁸³ to form a salt-bridge interaction (Fig. 2).

8-Hydroxyquinolines can exert their physiological properties through bidentate chelation of metal ions.¹¹ Since metal ions are important cofactors of many physiologically active enzymes, 8-hydroxyquinolines, have been explored as a viable drug discovery platform in many instances.¹² We envisioned the same premise in this particular instance since iron is essential for the activity of EGLN-1.

According to our modeling experiments (see the references and notes section), the 8-hydroxyquinoline **4** can coordinate iron via the amide carbonyl and the 8-OH, while the carboxylate interacts with Arg³⁸³ in the active site (Fig. 3). The quinoline ring likely stacks with Tyr³¹⁰ at the top of the active site.

Quinoline analogs were synthesized via a reaction between corresponding amines and the acid chloride of the 8-hydroxyquinoline-7-carboxylic acid. Good yields were obtained via the coupling between the acid chloride and the corresponding amine/aniline, while other coupling reagents (CDI, HBTU, HATU, and EDAC) gave poor yields (Scheme 1).

The biological activity of the 8-hydroxyquinolines derived against EGLN-1 enzyme and subsequent VEGF induction is described in the tables below. The 8-hydroxyquinoline-7-carboxylic acid was completely inactive (Table 1, Compound 1), while introduction of

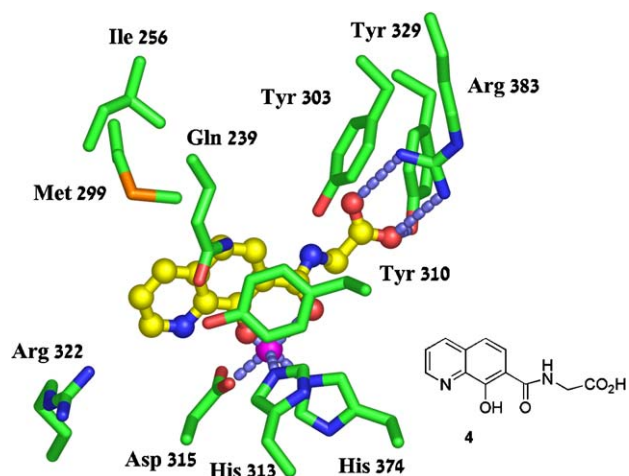
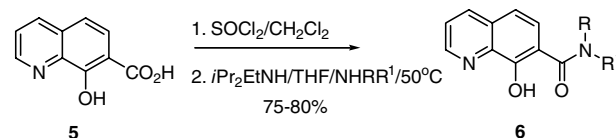


Figure 3. Predicted binding of compound **4** to the active site of EGLN-1. Only the most important interactions are shown.



Scheme 1.

the side chains bearing carboxylic acid (Table 1, Compound 1) delivered analog with good activity against EGLN-1. Interestingly, the corresponding naphthalene derivative had marginal activity (26.8 μ M) showing the importance of quinoline nitrogen. Next, we examined the possibility of replacing the carboxylic acid moiety with a suitable functional group that is smaller in size. *N*-(cyanomethyl)-8-hydroxy-7-carboxamide (Table 1, Compound 3) showed good activity comparable to its carboxylic acid counterpart. This was significant in improving the pharmacokinetic profile, particularly regarding membrane permeation in subsequent cellular assays.

The next direction of our SAR studies was focused on the analogs derived from the coupling between the 8-hydroxyquinoline-7-carboxylic acid and various substituted benzylamines. Upon examining the binding mode as predicted by the FlexX program, the potential cation- π interaction between the distal phenyl group and Arg³²² at the entrance of the active site (Fig. 4) struck us as interesting. The π -cation interaction which is the electrostatic interaction between a cation and the negative electrostatic potential associated with the face of a

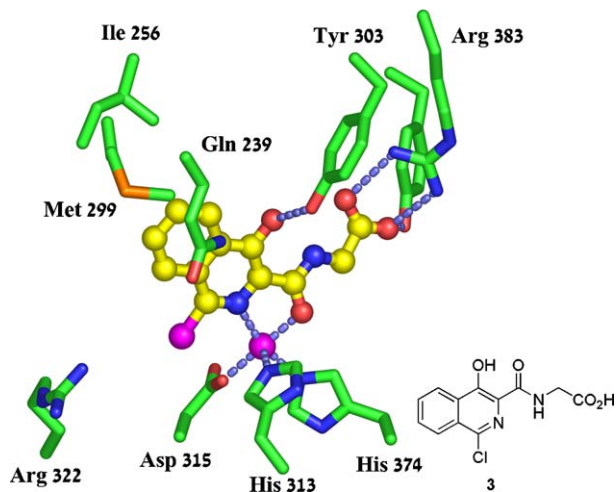
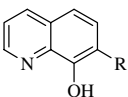
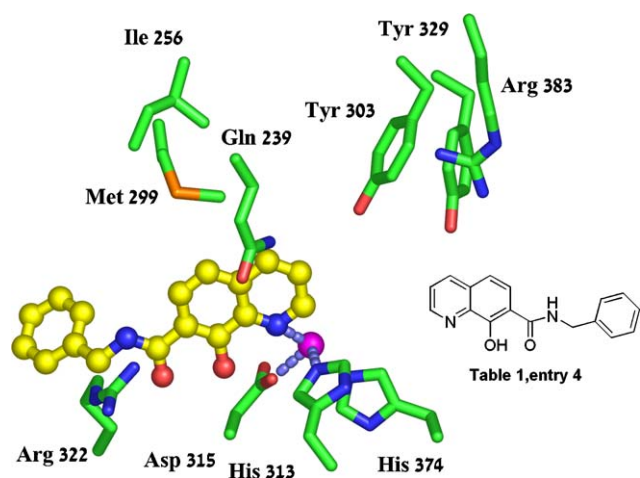


Figure 2. Binding of compound **3** to the active site of EGLN-1. Only the most important interactions are shown.

Table 1. SAR of 8-hydroxyquinoline derivatives (95% CI)

					
Compound	R	EGLN IC ₅₀ (μM)	Compound	R	EGLN IC ₅₀ (μM)
1		>100	11		9.7
2		5.0	12		3.9
3		4.4	13		6.1
4		4.2	14		4.1
5		4.6	15		10
6		4.8	16		3.2
7		7.4	17		7.2
8		4.4	18		5.3
9		28.7	19		6.9
10		6.0	20		5.8

**Figure 4.** Predicted binding of 8-hydroxyquinoline derivative (Table 1, Compound 4) to the active site of EGLN-1. Only the most important interactions are shown.

simple π system is a fairly new hypothesis and is argued as an important non-covalent interaction in biological recognition.¹³ In contrast to the binding mode of **4** (Fig. 3), in this instance, the quinoline nitrogen coordinates the iron. It is likely that the 8-hydroxyl is also involved in coordination, even though the present model positions it too far from the metal ion.

Earlier, we have regarded the interaction between the ligands and the active site as mostly lipophilic in nature (the active site consists of more lipophilic residues than hydrophilic residues). The unsubstituted benzamide analog (Table 1, Compound 4) showed good activity while substitutions at the 4-position of the phenyl ring with both electron-donating (Table 1, Compound 5) and electron-withdrawing groups (Table 1, Compound 6) generated compounds with comparable activity. The benzyl ester derivative (Table 1, Compound 11) showed

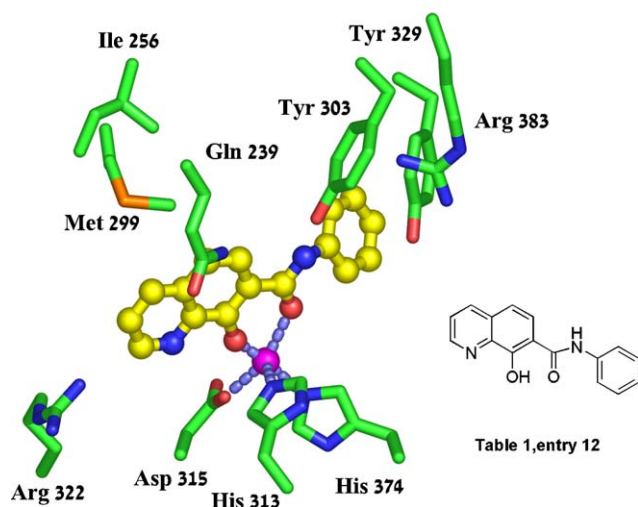


Figure 5. Predicted binding of 8-hydroxyquinoline derivative (Table 1, Compound 12) to the active site of EGLN-1. Only the most important interactions are shown.

reduced activity thus underlining the importance of amide functionality at this position Figure 5.

Next, we investigated the aniline-derived analogs: modeling studies revealed that these compounds may bind so that the distal phenyl ring of the side-chain points toward the active-site Arg383. The 8-hydroxyl and the amide carbonyl groups probably coordinate iron in a manner similar to that of compound 4 (Fig. 3). Hetero-aromatics may also be used instead of the phenyl group (Table 1, Compound 14). Interestingly, *N*-(3,5-dimethoxyphenyl)-8-hydroxyquinoline-7-carboxamide (Table 1, Compound 16) is twofold more active than the corresponding *N*-(3,5-dimethoxybenzyl)-8-hydroxyquinoline-7-carboxamide (Table 1, Compound 7) suggesting that the compound extension is limited by the depth of the binding site.

The analogs derived from phenethyl amines (Table 1, Compounds 19–22) also exhibited good activity (Fig. 6). Modeling suggested that these compounds bind

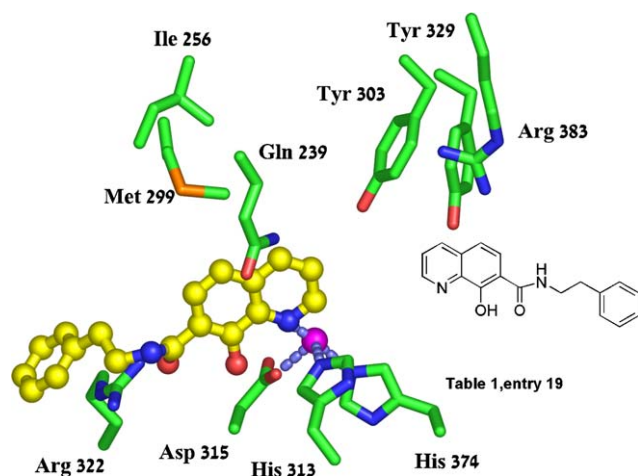


Figure 6. Predicted binding of 8-hydroxyquinoline derivative (Table 1, Compound 19) to the active site of EGLN-1. Only the most important interactions are shown.

to the enzyme in a mode similar to that of the benzylamine analogs (Fig. 4). A similar π -cation interaction with Arg322 was predicted for the distal phenyl group extending from the quinoline nucleus (Fig. 6).

Most of these 8-hydroxyquinoline analogs are potent inducers of VEGF (a downstream biomarker for HIF-1 stabilization). The most potent compound (Table 2, Compound 14) has an EC_{50} of 140 nM. In addition, several other analogs exhibited potent activity in the nanomolar range. In summary, we were able to design and synthesize novel HIF-1 α prolyl hydroxylase inhibitors with the aid of the X-ray structure of EGLN-1 catalytic domain in complex with a potent inhibitor. Our compounds were shown to be potent VEGF inducers in a cell-based assay. Currently, these 8-hydroxyquinoline carboxamides are undergoing selectivity and PK studies.

Modeling studies. The 3D coordinates of receptor were directly adapted from the in-house X-ray structure of human EGLN-1. The 3D structures of compounds to be docked were generated and minimized by Sybyl 7.9 (Sybyl; Tripos Inc., 1699 South Hanley Rd, St. Louis, MO 63144, USA). The protonation state of each compound was assigned based on physiologic condition. For instance, all carboxylic acids were deprotonated. All docking calculations were performed by using FlexX (FlexX; Tripos Inc., 1699 South Hanley Rd, St. Louis, MO 63144, USA) with standard docking procedure and parameters. The active site is defined as the collection of amino acids lying within 6.5 Å of atoms of compound 3 determined by the in-house X-ray structure. FlexX is a fragment-based docking program. The docking conformations were ranked by using FlexX scores. The final protein–ligand complexes were not minimized after the docking. With the same docking setup, we were able to successfully reproduce the binding conformation of compound 3 to EGLN-1. In the predicted protein–ligand complex with the best FlexX score, the RMSD (Root Mean Square Deviation) between the coordinates of the predicted ligand and those of the cocrystal ligand is less than 1.5 Å.

EGLN-1 activity assay. The EGLN-1 enzyme activity was determined using mass spectrometry (matrix-assisted laser desorption ionization, time-of-flight MS, MALDI-TOF-MS).¹⁴ The HIF-1 α peptide corresponding to residues 556–574 (DLDLEALAPYIPADDDFQL) was used as substrate. The reaction was conducted in a total volume of 50 μ L containing Tris–Cl (5 mM, pH 7.5), ascorbate (120 μ M), 2-oxoglutarate (3.2 μ M), HIF-1 α (8.6 μ M), and bovine serum albumin (0.01%). EGLN-1, quantity predetermined to hydroxylate 20% of substrate in 20 min, was added to start the reaction. Where inhibitors were used, compounds were prepared in dimethylsulfoxide at 10-fold final assay concentration. After 20 min at room temperature, the reaction was stopped by transferring 10 μ L of reaction mixture to 50 μ L of a mass spectrometry matrix solution (α -cyano-4-hydroxycinnamic acid, 5 mg/ml in 50% acetonitrile/0.1% TFA, 5 mM NH_4PO_4). Two microliters of the mixture was spotted onto a MALDI-TOF-MS target

Table 2. VEGF activity of 8-hydroxyquinoline derivatives (95% CI)

Compound	R	VEGF EC ₅₀ (μM)	Compound	R	VEGF EC ₅₀ (μM)
1		>100	11		>100
2		4.1	12		0.14
3		0.89	13		0.42
4		0.62	14		1.9
5		3.1	15		>100
6		—	16		3.2
8		0.89	17		0.58
9		—	18		—
10		0.63	19		—
			20		—

plate for analysis with an Applied Biosystems (Foster City, CA) 4700 Proteomics Analyzer MALDI-TOF-MS equipped with a Nd:YAG laser (355 nm, 3 ns pulse width, 200 Hz repetition rate). Hydroxylated peptide product was identified from substrate by the gain of 16 Da. Data defined as percent conversion of substrate to product were analyzed in GraphPad Prism 4 to calculate IC₅₀ values.

VEGF ELISA. HEK293 cells were seeded in 96-well poly-lysine coated plates at 20,000 cells per well in DMEM (10% FBS, 1% NEAA, and 0.1% glutamine).

Following overnight incubation, the cells were washed with 100 μL of Opti-MEM (Gibco, Carlsbad, CA) to remove serum. Compound in DMSO was serially diluted (beginning with 100 μM) in Opti-MEM and added to the cells. The conditioned media were analyzed for VEGF with a Quantikine human VEGF immunoassay kit (R&D Systems, Minneapolis, MN). Optical density measurements at 450 nm were recorded using the Spectra Max 250 (Molecular Devices, Sunnyvale, CA). Data defined as % of DFO stimulation were used to calculate EC₅₀ values with GraphPad Prism 4 software.

References and notes

- Mack, C. A.; Magovern, C. J.; Budenbender, K. T.; Patel, S. R.; Schwatz, E. A.; Zanzonico, P.; Ferris, B.; Sanborn, T.; Isom, O. W.; Crystal, R. G.; Rosengart, T. K. *J. Vasc. Surg.* **1998**, 27, 699.
- Bruick, R. K.; McKnight, S. L. *Genes Dev.* **2001**, 15, 2497.
- Safran, M.; Kaelin, W. G., Jr. *J. Clin. Invest.* **2003**, 111, 779.
- Semenza, G. L. *J. Appl. Physiol.* **2000**, 88, 1474.
- Semenza, G. L. *Cell* **2001**, 107, 1.
- Kondo, K.; Kaelin, W. G., Jr. *Exp. Cell. Res.* **2001**, 264, 117.
- Semenza, G. *Biochem. Pharmacol.* **2002**, 64, 993.
- (a) McDonough, M. A.; McNeill, L. A.; Tilliet, M.; Papamicaël, C. A.; Chen, Q.-Y.; Benerji, B.; Hewitson, K. S.; Schofield, C. J. *J. Am. Chem. Soc.* **2005**, 127, 7680; (b) Mole, D. R.; Schlemminger, I.; McNeill, L. A.; Hewitson, K. S.; Pugh, C. W.; Ratcliffe, P. J.; Schofield, C. J. *Bioorg. Med. Chem. Lett.* **2003**, 13, 2677; (c) Schlemminger, I.; Mole, R.; McNeill, L. A.; Dhanda, A.; Hewitson, K. S.; Tian, Y.-M.; Ratcliffe, P. J.; Pugh, C. W.; Schofield, C. J. *Bioorg. Med. Chem. Lett.* **2003**, 13, 1451.
- Guenzler, -P.; Volkmar, K.; Stephen, J.; Liu, D. Y.; Todd, W. PCT. In. Appl. WO 2005007192, 2005.
- Evdokimov, A. et. al, *Nat. Struc. Biol.* **2006**, submitted for publication.
- Caris, C.; Baret, P.; Pierre, J.-L.; Serratrice, G. *Tetrahedron* **1996**, 52, 4659.
- (a) Zhuang, L.; Wai, J. S.; Embrey, M.; Fisher, T. E.; Egbertson, M. S.; Payne, L. S.; Guare, J. P.; Vacca, J. P.; Hazuda, D. J.; Felock, P. J.; Wolfe, A. L.; Stillmock, K. A.; Witmer, M. V.; Moyer, G.; Schleif, W. A.; Gabyelski, L. J.; Leonard, Y. M.; Lynch, J. J.; Michelson, S. R.; Young, S. D. *J. Med. Chem.* **2003**, 46, 453; (b) Ujiiie, T. *Chem. Pharm. Bull.* **1975**, 23, 62; (c) Paris, D.; Cottin, M.; Demonchaux, P.; Augurt, G.; Dupassieux, P.; Lenoir, P.; Peck, M. J.; Jasserand, D. *J. Med. Chem.* **1995**, 38, 669.
- Zacharias, N.; Dougherty, D. A. *Trends Pharmacol. Sci.* **2002**, 23, 281.
- Greis, K. D.; Zhou, S.; Burt, T. M.; Carr, A. N.; Dolan, E.; Easwaran, V.; Evodokimov, A.; Kawamoto, R.; Rosegen, J.; Davis, G. F. *J. Am. Soc. Mass. Spectrom.* **2006**, 815.